Natural Resources for Human Health
eISSN: 2583-1194

Original Research

Received 14 April 2026
Revised 16 May 2026
Accepted 15 June 2026

Natural Resources for Human Health 2026, Vol. 6 (3s): 976–997

KEYWORDS:
Quadcopter, 6DOF, PID controller, Propeller, Planetary expedition

Design and Simulation of Quadcopter for Planetary Expedition

*Dr. Deepa S N[1], *Dr. Sowmyashree N[2], *Mr. Abhishek G[3], Mrs. Apoorvashree H L[4], Dr. Likhitha R[5], Shreepad Parameshwar Hangari[6]

[1]Assistant Professor, EEE, JSS Science and Technology University, Mysuru, India. Email: deepa.archak@jssstuniv.in
[2]Assistant Professor, EEE, JSS Science and Technology University, Mysuru, India. Email: sowmyashree2688@jssstuniv.in
[3]Assistant Professor, EEE, JSS Science and Technology University Mysuru, India. Email: abhishekg@jssstuniv.in
[4]Assistant Professor, EEE, GSSS Institute of Engineering and Technology for Women, Mysuru, India. Email: apoorvalingaraj@gmail.com
[5]Assistant Professor, EEE, Nitte Meenakshi Institute of Technology, Bengaluru, India. Email: likhitha.r@nmit.ac.in
[6]Student, EEE, JSS Science and Technology University, Mysuru, India. Email: shreepadphangari@gmail.com
*Corresponding authors

ABSTRACT: Quadcopters were also called as quadrotor helicopter, is popularly known as Unmanned Aerial Vehicles (UAV). Quadcopters have been widely used in much of the civilian and military applications over the past few years due to its compact size and high stability. Numerous studies are being conducted to investigate the potential for employing these devices for different operations, such as delivery of packages, construction work, hurricane hunting, 3D mapping, preserving wildlife, agricultural operations, search and rescue, etc. Since these devices are unmanned vehicles, the effectiveness of their navigation control system determines how well they operate. It is however difficult to design robust controller for such systems. This is due to the fact that quadcopters are highly sensitive to control inputs. The focus of this paper is to design body frame and simulation of a quadcopter for planetary expedition. It uses a linear proportional-derivative integral (PID) controller to control the quadcopter's altitude, attitude, direction, and location in space. The created control system uses six degrees of freedom (3 linear and 3 angular motions) to control both rectangular x, y, and z positions as well as orientation. The body components of the quadcopter are designed using AutoCAD and imported to Simulink/Matlab for assembly and performance evaluation considering the external environment with varying wind speed on earth and mars. The results revealed that the designed quadcopter was reliable and capable of adapting for exclusive wind disturbances.

1. INTRODUCTION

A helicopter with four rotors is referred to as a quadcopter or quadrotor. The quadcopter's rotors are arranged in a square pattern with equal spacing from the centre of mass and are oriented upward. By changing the angular velocities of the electric motor-driven rotors, the quadcopter may be maneuvered. Due to its straightforward construction, the quadcopter is a common design for micro unmanned aerial vehicles (UAVs). Quadcopters are employed in multiple applications, such as surveillance, search and rescue operations, aerial identification, architectural inspections, industrial monitoring duties, and payload delivery missions [1], [2].

A quadcopter can be remotely controlled by a human operator or function autonomously. Autonomous vehicles are driven by onboard computers programmed to perform either a narrow range of tasks or a broad set of operations. The quadrotor is a highly nonlinear, multivariable system with six degrees of freedom (DOF) but only four actuators, making it an underactuated system that presents significant challenges in control design [3]. Systems that are underactuated possess fewer control inputs than the system's degrees of freedom. Because of the nonlinear coupling between the actuators and the degrees of freedom, they are inherently difficult to control. Researchers have devoted considerable attention to quadcopters because of their complex dynamics, resulting in extensive investigations in modeling, control, navigation, and autonomous operation. Most studies begin with the fundamental dynamic model of the quadcopter, while more sophisticated aerodynamic effects have also been incorporated to improve model fidelity [4], [5]. Various control strategies have been explored, including PID controllers [6]–[9], backstepping controllers [3], [10], nonlinear controllers [11], linear quadratic regulator (LQR) controllers [9], and nonlinear controllers with layered saturations [12], [13]. These control approaches rely on accurate position and attitude measurements obtained from sensors such as gyroscopes, accelerometers, GPS modules, sonar sensors, and laser-based systems [14], [15].

In this paper, a PID-based control system is designed to regulate the six degrees of freedom of a quadrotor, comprising three translational motions (x, y, and z) and three rotational motions (roll, pitch, and yaw). The mathematical model of the 6-DOF quadrotor system is developed by considering both velocity and acceleration vectors, resulting in a nonlinear model that closely represents the real system. The model is derived using the Euler–Newton formulation to describe the three-dimensional motion of the rigid body [16]. The structural components of the quadcopter are designed using AutoCAD, while the overall prototype is modeled and developed in MATLAB/Simulink using PID control techniques [17], [18].

Unlike conventional studies that focus solely on quadcopter stabilization, this work presents a mission-oriented simulation framework for planetary exploration. The proposed framework integrates a 6-DOF nonlinear dynamic model, a custom-designed FlameWheel-450-based airframe, PID-based trajectory tracking and attitude stabilization, and environmental modeling for Earth and Mars conditions. The performance of the designed quadcopter is evaluated under varying environmental parameters including gravitational acceleration, atmospheric density, aerodynamic drag, ambient temperature, payload conditions, and wind disturbances. Furthermore, the study investigates the suitability of the proposed platform for planetary sample collection missions by analyzing trajectory tracking capability, payload handling, and flight stability under Earth and Mars operating environments. This provides a preliminary feasibility assessment methodology for quadcopter-based planetary exploration systems.

2. DESIGN OF QUADCOPTER FOR PLANETARY EXPEDITION

2.1 Quadcopter Configuration and Flight Dynamics

A quadcopter features four propellers, that are setup either in a cross or plus configuration for flight. It is a huge advantage for the quadcopter to be able to take off and land vertically since it reduces the need for a landing platform. Additionally, it enables the quadcopter to hover in a place with considerable stability. The quadcopter's hover stability manages to keep it from crashing in the instance of a strong wind or owing to its weight.

The quadcopter's six degrees of freedom are depicted in Fig. 1. In Fig. 1(a) x and y indicate translational motion along the x and y-axes, respectively, and ψ represents yaw, the rotating motion about the z-axis. In contrast, ϕ represents roll, the rotational motion about the x-axis, θ represents pitch, the rotational motion about the y-axis, and z represents translational motion in the direction perpendicular to the ground. The front propeller is indicated with the label as 1.

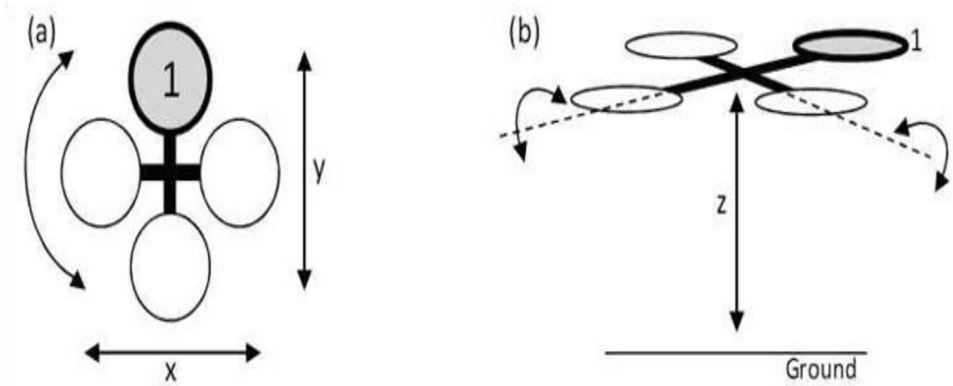

Fig. 1: The six degrees of freedom of the quadcopter.

The quadcopter may hover using a hover control unit at a fixed height z (Fig. 1(b)), with the gyroscope stabilizing the roll and pitch angles. The degree of difficulty will drop from six to only three since the operator at the command base will only need to regulate the quadcopter's movement along the x- and y-axes and its rotation about the z-axis. Despite having six degrees of freedom (DOF), the quadcopter only has four propellers. Due to the structure of the quadcopter, the four best controllable variables connected to the four fundamental movements that enable the quadcopter to achieve a specific height and attitude may be selected such as throttle, roll, pitch and yaw.

2.2 Frame Architecture and Material Specifications

In this paper the body frame of quadcopter has been designed as per the specifications of FlameWheel 450 (F450) which is a multi-rotor designed body frame. This can achieve hovering, cruising, even rolling and other flight elements. It can also be applied for aerial photography, FPV and other aero-modeling activities. The dimension of the body frame, top and bottom plate, cap and propeller system, BLDC motor designed dimension of quadcopter for planetary expedition is as shown in Fig. 2.

The proposed quadcopter frame is based on the FlameWheel 450 (F450) platform, which is widely adopted in UAV applications because of its lightweight structure, mechanical robustness, and ease of integration with flight control systems. In practical implementations, F450-type frames are commonly fabricated using glass-fibre reinforced nylon and carbon-fibre composite materials due to their high strength-to-weight ratio, corrosion resistance, and vibration damping characteristics. Such lightweight composite materials are particularly advantageous for planetary exploration missions, where maximizing payload capacity and flight endurance is critical. The present work focuses primarily on dynamic modelling and flight-performance evaluation; therefore, detailed finite-element structural analysis of the frame is beyond the scope of this study and is considered as future work [19], [20].

Natural Resources for
Human Health
eISSN: 2583-1194

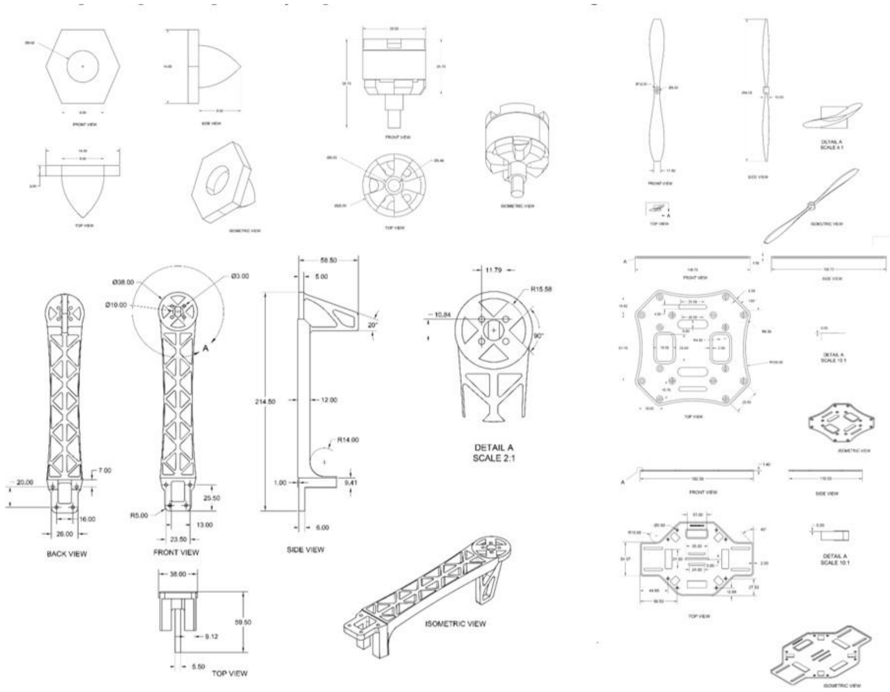

Fig. 2: The designed body dimensions of the quadcopter for planetary expedition.

2.3 Six-Degree-of-Freedom Dynamic Model

The quadcopter is modeled as a rigid body with six degrees of freedom (6-DOF), consisting of three translational coordinates (*x, y, z*) and three rotational coordinates (ϕ, θ, ψ), representing the roll, pitch, and yaw angles, respectively. The translational dynamics are governed by Newton's second law:

$$m\ddot{x} = U_1(\cos\phi \sin\theta \cos\psi + \sin\phi \sin\psi) \tag{1}$$

$$m\ddot{y} = U_1(\cos\phi \sin\theta \sin\psi - \sin\phi \cos\psi) \tag{2}$$

$$m\ddot{z} = U_1 \cos\phi \cos\theta - mg \tag{3}$$

where m is the mass of the quadcopter, g is the gravitational acceleration, and U_1 is the total thrust generated by the four rotors.

The rotational dynamics are expressed using Euler's rotational equations:

$$I_x\ddot{\phi} = (I_y - I_z)\dot{\theta}\,\dot{\psi} + U_2 \tag{4}$$

$$I_y\ddot{\theta} = (I_z - I_x)\dot{\phi}\,\dot{\psi} + U_3 \tag{5}$$

$$I_z\ddot{\psi} = (I_x - I_y)\dot{\phi}\,\dot{\theta} + U_4 \tag{6}$$

The control inputs are defined as

$$U_1 = k_f(\omega_1^2 + \omega_2^2 + \omega_3^2 + \omega_4^2) \tag{7}$$

$$U_2 = lk_f(\omega_4^2 - \omega_2^2) \tag{8}$$

$$U_3 = lk_f(\omega_3^2 - \omega_1^2) \tag{9}$$

$$U_4 = k_m(\omega_1^2 - \omega_2^2 + \omega_3^2 - \omega_4^2) \tag{10}$$

where I_x, I_y, and I_z denote the moments of inertia about the body-fixed axes, l is the distance from the center of mass to each rotor, k_f is the thrust coefficient, k_m is the drag coefficient, and ω_i is the angular velocity of the i-th rotor.

The complete nonlinear 6-DOF dynamic model used for simulation and controller design is fully described by (1)–(10).

3. Simulation of Quadcopter for Planetary Expedition

In order to implement the formulated quadcopter dynamics equations in Simulink, a level-2 M-file S-function API (application programming interface) is used. This function allows using Matlab scripting language to create Simulink custom blocks and specify their properties and behavior. All the formulated equations mentioned in the previous chapter are written in Matlab script and linked to quadcopter block as shown in Fig. 3.

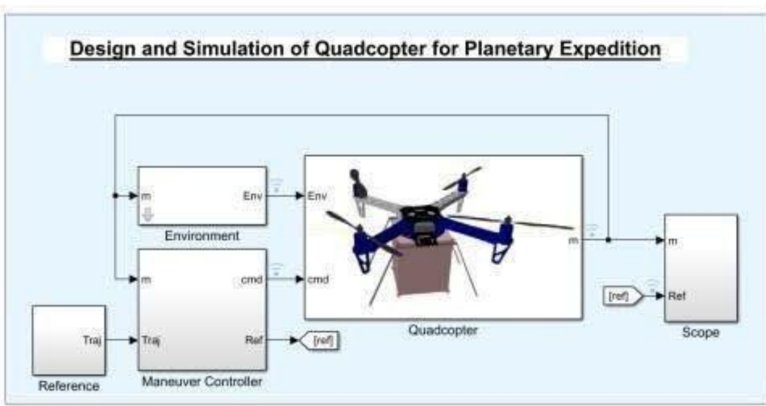

Fig. 3: Simulink model of Quadcopter.

The maneuver control block shown in Fig. 4 implements the flight control strategy adopted for the proposed quadcopter. The controller is responsible for regulating the position, altitude, roll, pitch, and yaw motions of the vehicle while generating the corresponding motor thrust commands required for trajectory tracking and attitude stabilization.

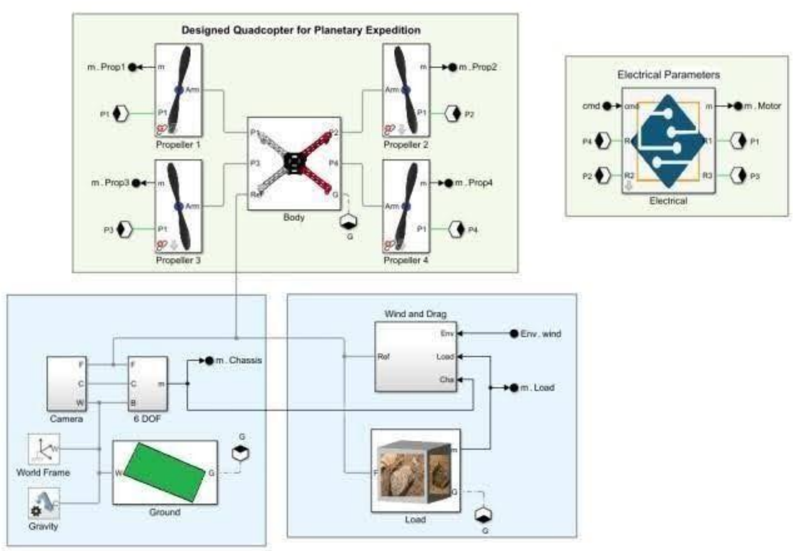

Fig. 4: Maneuver control block of quadcopter.

A cascaded PID control architecture is employed for position and attitude stabilization of the quadcopter owing to its simplicity, low computational complexity, and proven effectiveness in UAV applications [17], [18]. The controller gains were determined through an iterative tuning procedure in MATLAB/Simulink. Initially, the proportional gains were adjusted to obtain a satisfactory transient response, followed by derivative gain tuning to improve damping characteristics and suppress oscillations. Finally, the integral gains were selected to minimize steady-state tracking errors. The tuning objective was to achieve stable take-off, fast settling time, minimum overshoot, accurate trajectory tracking, and satisfactory disturbance rejection under varying wind conditions. The tuning process was repeated for both Earth and Mars environmental scenarios to ensure acceptable closed-loop performance throughout the simulation studies.

The Fig. 5a illustrates the designed and assembled quadcopter with body frame and propeller system for planetary expedition along with the blocks of 6 degrees of freedom, wind and drag, camera, ground, gravity, load and electrical parameters. Fig. 4 shows the maneuver control block of quadcopter for controlling position, altitude, yaw, pitch, roll of quadcopter and motor mixer for thrust command. Fig. 5b depicts the Simulink model of quadcopter's propeller evaluation considering the control parameters.

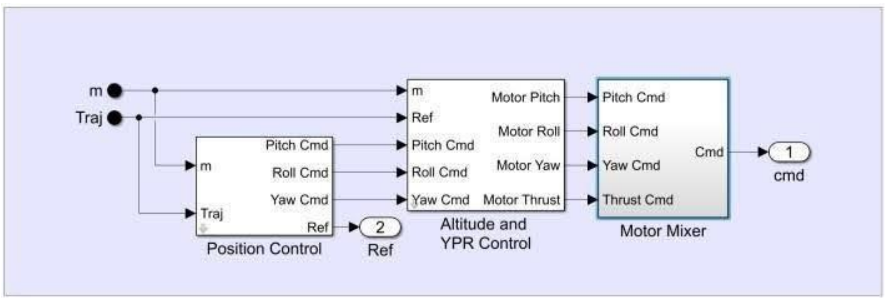

(a) Simulink model of assembled quadcopter.

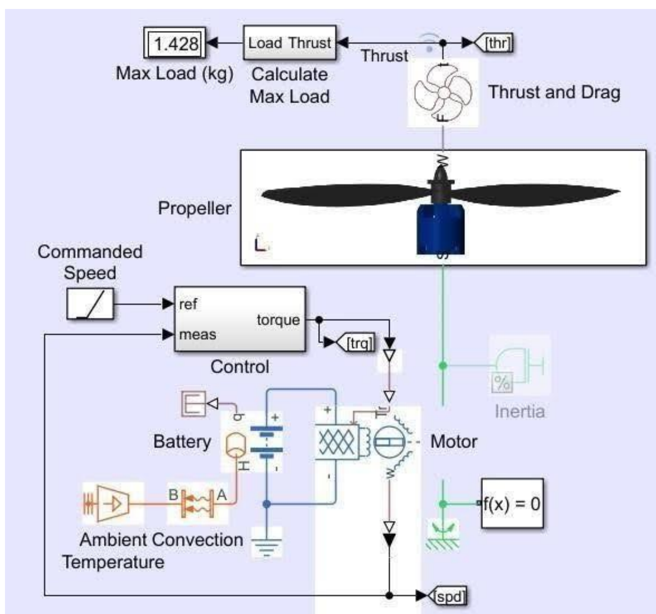

(b) Simulink model to calculate maximum loading capacity of quadcopter.

Fig. 5: Simulink models used for planetary expedition analysis.

3.1 Mars Environmental Assumptions

The environmental parameters used in the Mars simulation are based on publicly available planetary data reported by NASA and related planetary science literature [21], [22]. Compared to Earth, Mars possesses significantly lower atmospheric density and gravitational acceleration, which directly influence aerodynamic lift generation, vehicle stability, and payload-carrying capability. The environmental parameters adopted in this study are summarized in Table I.

TABLE I: Environmental Parameters Used for Earth and Mars Simulations

Parameter	Earth	Mars
Gravity (m/s^2)	9.81	3.71
Atmospheric Density (kg/m^3)	1.225	0.020
Mean Surface Pressure (Pa)	101,325	610
Average Temperature (°C)	25	–63

The significantly lower atmospheric density on Mars reduces the aerodynamic thrust generated by conventional propellers. Consequently, larger propeller diameters and higher rotational speeds are generally required to produce sufficient lift. The adopted simulation parameters enable a preliminary assessment of quadcopter flight performance under representative Martian operating conditions.

4. Results and Discussion

The performance evaluation of designed quadcopter was carried out for the external environment of earth and mars considering its air resistance, ambient temperature, gravity and varied wind speed. The trajectory path for quadcopter to move along the reference path was pre-defined by using spline points and waypoints. The evaluating criteria was such that initially the quadcopter has to take off from its starting point with the required thrust carrying the load and move along the predefined spline points to the destination point with controlled pitch, yaw and roll. Then it has to drop off the carried load to the ground and get back to the initial point. The evaluating parameters are as follows,

- Positions and velocities of quadcopter chassis
- Trajectory of quadcopter in 3D space
- Current flow to BLDC motors and battery SOC
- Thrust, speed and torque of quadcopter propeller

4.1 Performance Evaluation of Quadcopter in Earth's Environment

The following control parameters had been implemented to create earth's environment for the designed quadcopter to fly and number of cases has been considered to evaluate its performance by varying the wind speed.

Case I – Earth's Environment:

```
propeller.Kthrust = 0.1072;      % N
air_rho          = 1.225;       % kg/m^3
air_temperature  = 273+25;      % K
gravity          = 9.80665;     % m/s^2
wind_speed       = 0;           % (m/s)
trajectory_path  = round_trip_1;
```

Fig. 6a shows the plot of positions and velocities of quadcopter chassis when the Case I control parameters were executed. The first column plots show the position of the quadcopter with respect to the xyz plane, the second column represents the velocity of the quadcopter in the xyz plane, and the third column represents the roll, yaw, and pitch of the quadcopter. The red solid line represents the reference value and the blue solid line represents the measured value. Fig. 6b shows the actual quadcopter trajectory in 3D space. It can be observed that the quadcopter traced the predefined path for zero wind speed and was able to reach the destination and return to its initial position.

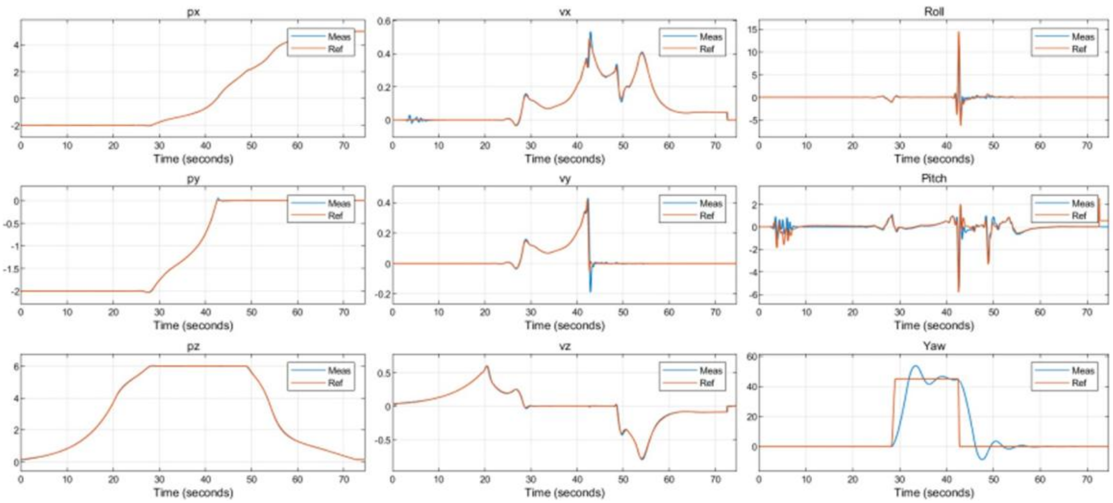

(a) Plot of positions and velocities of quadcopter chassis.

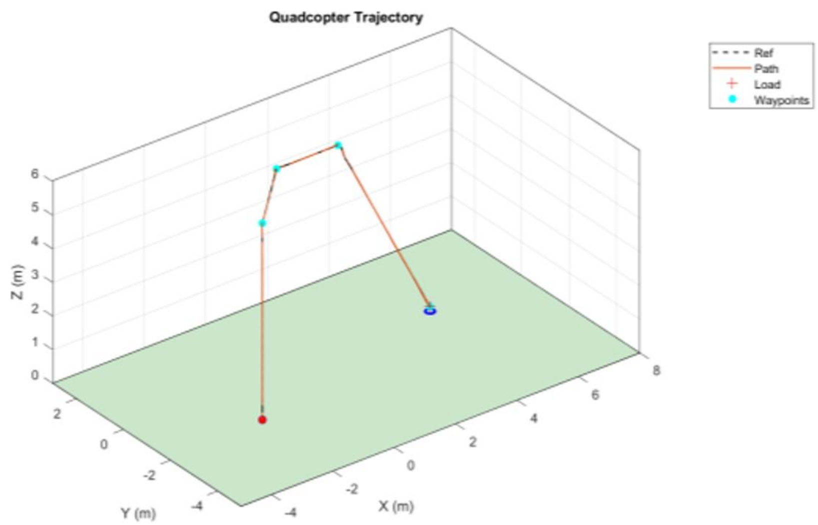

(b) Trajectory of quadcopter in 3D plane.

Fig. 6: Plot of positions and velocities of the quadcopter chassis and its trajectory in the 3D plane for Case I – Earth's environment.

Fig. 7a shows the measured battery SOC and battery temperature. It is evident that the battery charge reduced more rapidly while carrying a load (simulation time: 0–75 s) than during the unloaded condition (simulation time: 75–150 s). A similar trend is observed in the battery temperature. Fig. 7b shows the thrust developed by the propeller system of the quadcopter. It can be seen that the thrust required by the quadcopter is greater when carrying a payload than when operating without a payload under the same environmental conditions.

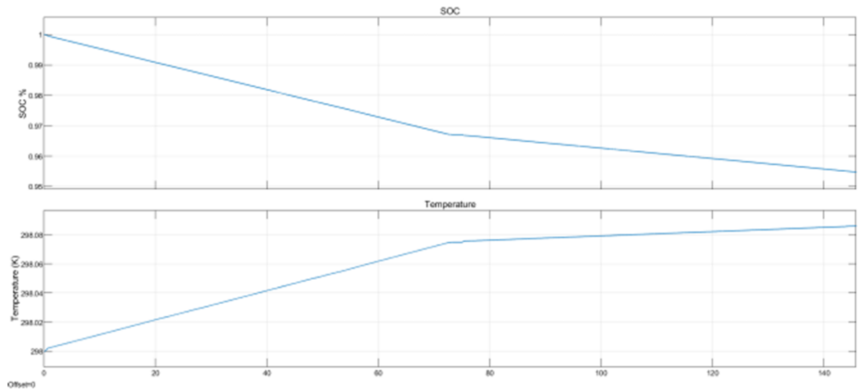

(a) Measured battery SOC and battery temperature.

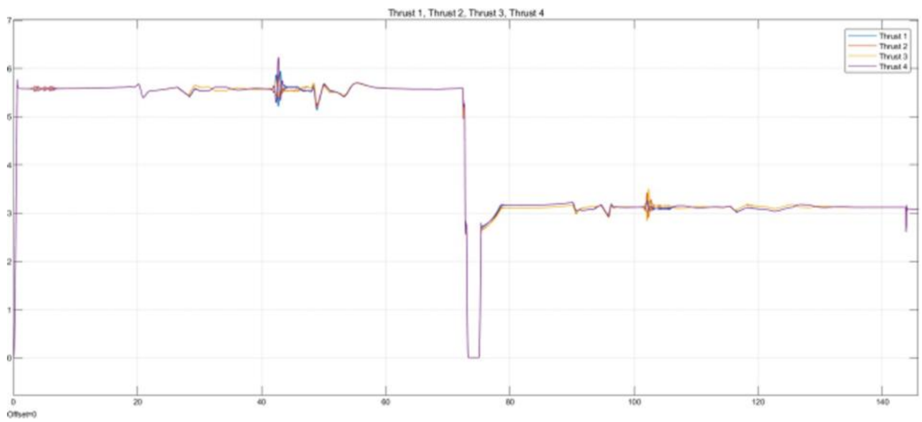

(b) Thrust developed by the propeller system.

Fig. 7: Measured battery SOC, battery temperature, and thrust developed by the propeller system of the quadcopter for Case I – Earth's environment.

It was evident from the above performance evaluation that the quadcopter successfully traced the predefined path under zero wind-speed conditions. The vehicle reached the destination, delivered the payload, and returned to its initial position while accurately following the commanded trajectory.

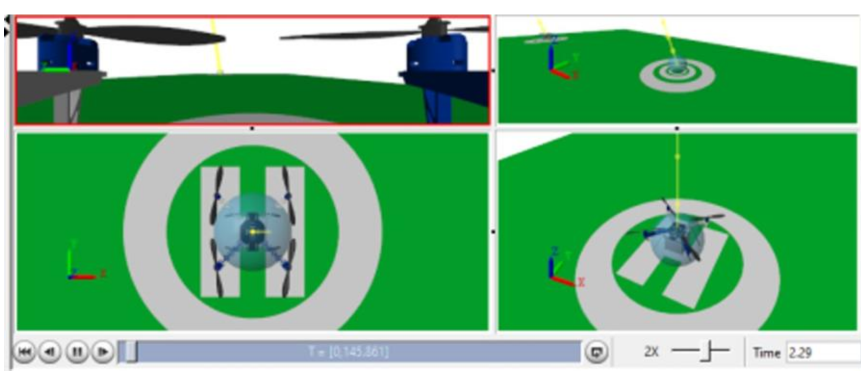

(a) Initial take-off and stabilization.

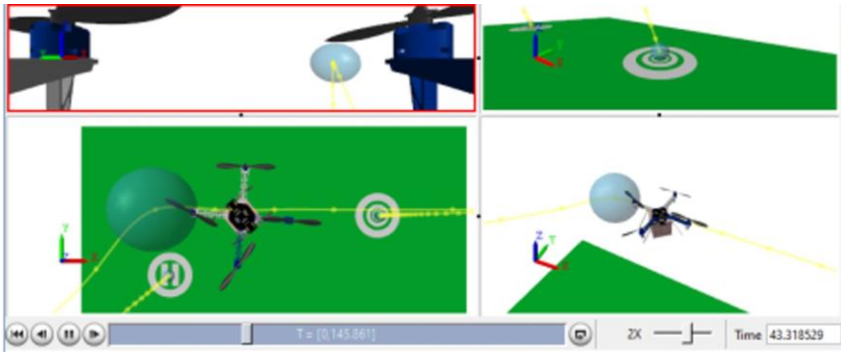

(b) Payload transportation.

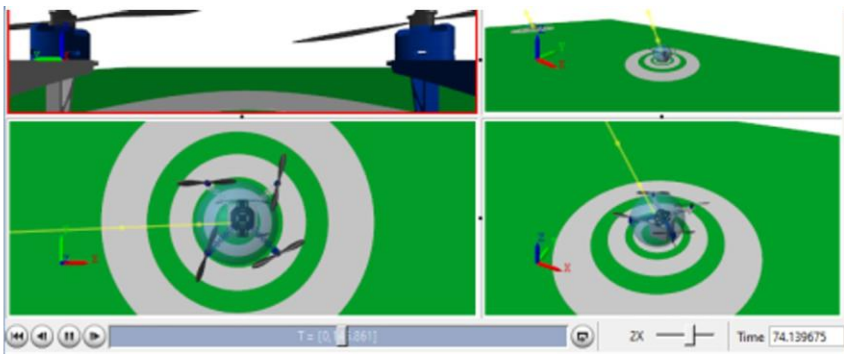

(c) Landing and mission completion.

Fig. 8: Visualization of the quadcopter performance for Case I.

Case II – Earth's Environment:

propeller.Kthrust = 0.1072; % N

air_rho = 1.225; % kg/m^3

air_temperature = 273+25; % K

gravity = 9.80665; % m/s^2

wind_speed = 20; % (m/s)

trajectory_path = round_trip_2;

Fig. 9a shows the plot of positions and velocities of quadcopter chassis when the Case II control parameters was executed. Fig. 9b shows the actual quadcopter trajectory in 3D plane tracing the predefined path and can be seen that there was lot of wobbling and deviation in the actual quadcopter trajectory due to increased wind speed and was not able to reach the destination and flip out from the reference path.

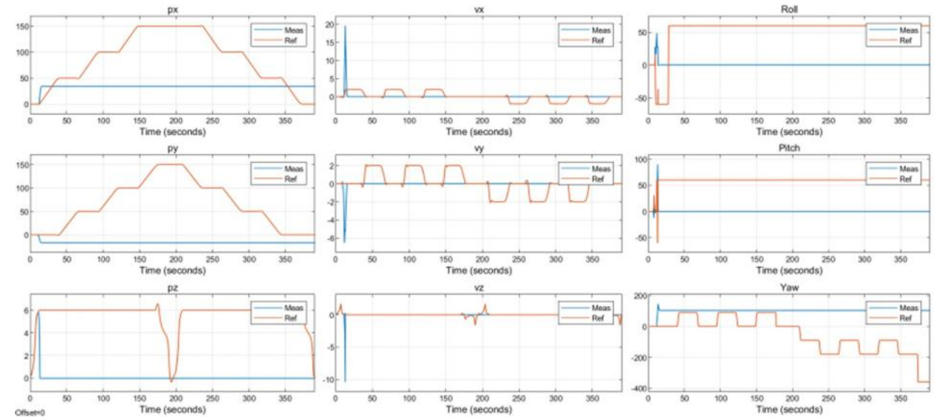

(a) Plot of positions and velocities of quadcopter chassis.

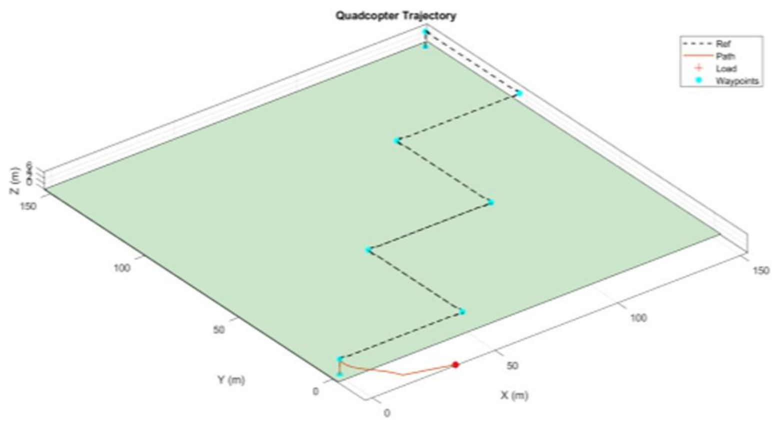

(b) Trajectory of quadcopter in 3D plane.

Fig. 9: Plot of positions and velocities of quadcopter chassis and its trajectory in 3D plane for Case II – Earth's environment.

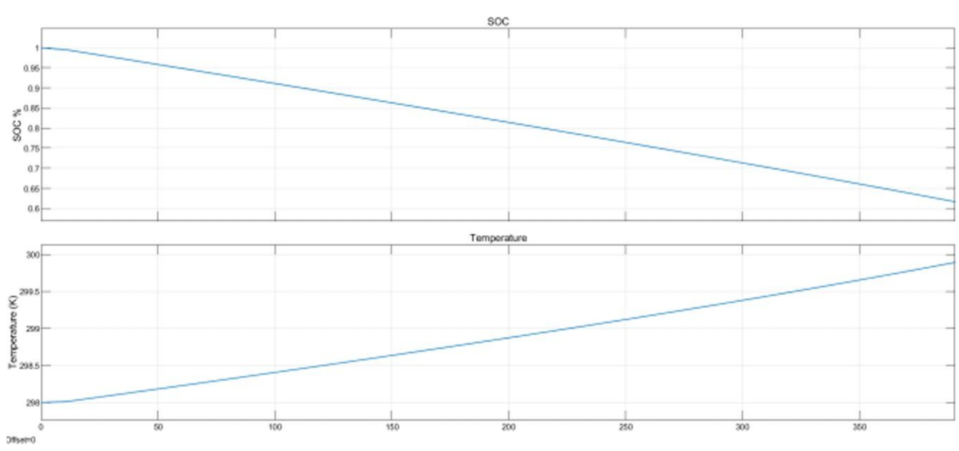

(a) Measured battery SOC and battery temperature.

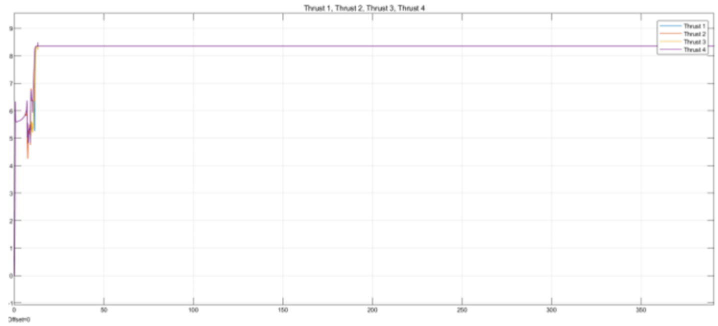

(b) Thrust developed by the propeller system.

Fig. 10: Measured battery SOC, battery temperature and thrust developed by the propeller system of quadcopter for Case II – Earth's environment.

It was proved from the above quadcopter performance evaluation that it didn't trace the pre-defined path and can be seen that there was lot of wobbling and deviation in the actual quadcopter trajectory due to increased wind speed and was not able to reach the destination and flip out from the reference path in spite of taking all commands given and interpreted. Hence it was evident from the above performance evaluation that the designed quadcopter was capable of carrying load to the destination point in presence of variable wind speed up to 15 m/s in earth's environment wherein for the predefined paths taken as per number of cases considered. Beyond that the quadcopter wasn't reach the destination due to presence of excessive wind resulted in wobbling and flip out from the reference path.

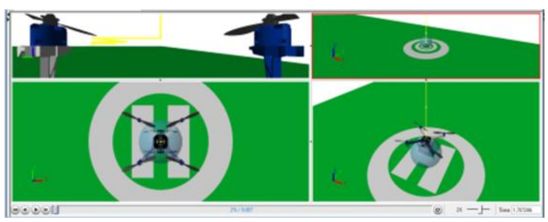

(a) Initial flight condition.

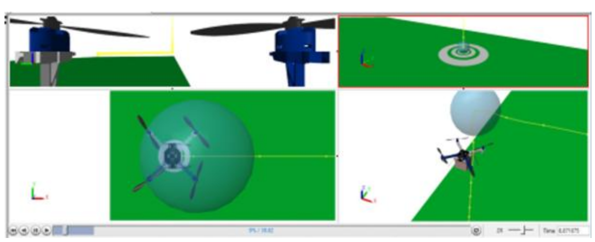

(b) Mid-flight condition.

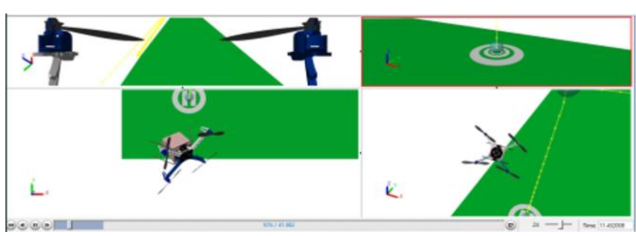

(c) Final flight condition.

Fig. 11: Visualization of performance of quadcopter for Case II.

4.2 Evaluation of Designed Quadcopter Propeller for Earth's Environment

Figure 12a shows the plot of propeller harness test indicating the speed, torque and thrust developed by the propeller system of the designed quadcopter for earth. It was observed that as and when the propeller stars to rotate, its speed, torque and thrust were gradually increased and attains a stable state in order to move the quadcopter to the required location. It was evident from the Figure 12b that the calculated maximum load of 2.136 kg can be carried by the designed quadcopter in the earth environment as per the performance evaluation.

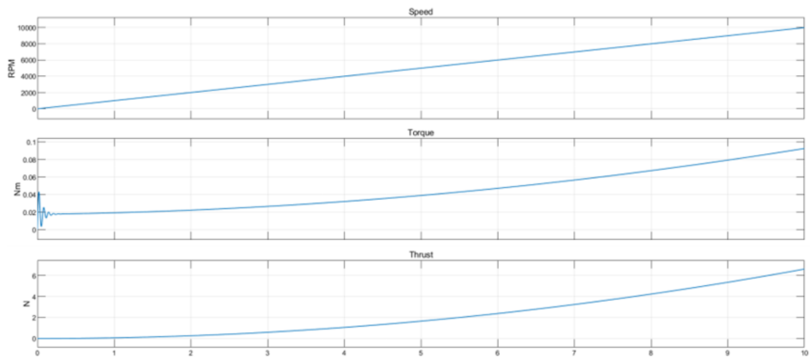

(a) Propeller harness test showing speed, torque and thrust characteristics.

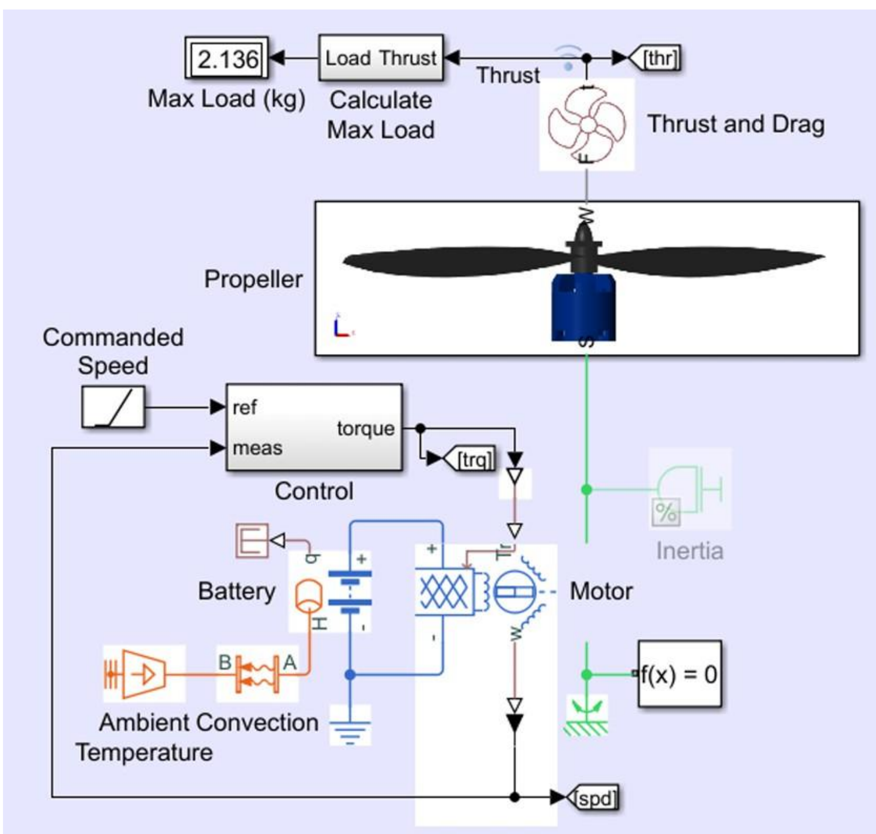

(b) Simulink model used to calculate the maximum loading capacity of the quadcopter.

Fig. 12: Propeller evaluation and maximum loading capacity of the designed quadcopter in Earth's environment.

eISSN: 2583-1194

4.3 Performance Evaluation of Quadcopter in Mars Environment

The following control parameters had been implemented to create mars environment for the designed quadcopter to fly and number of cases was considered to evaluate its performance by varying the wind speed.

Case I – Mars Environment:

propeller.Kthrust = 2.872;   % N

air_rho   = 0.020;   % kg/m^3

air_temperature = 273-63;   % K

gravity   = 3.721;   % m/s^2

wind_speed   = 0;   % (m/s)

trajectory_path = round_trip_1;

Fig. 13a shows the plot of positions and velocities of quadcopter chassis when the Case I control parameters was executed. Fig. 13b shows the actual quadcopter trajectory in 3D plane tracing the predefined path and can be seen that there was no deviation in the actual quadcopter trajectory due to zero wind speed but still it was able to reach the destination and return to its original position successfully.

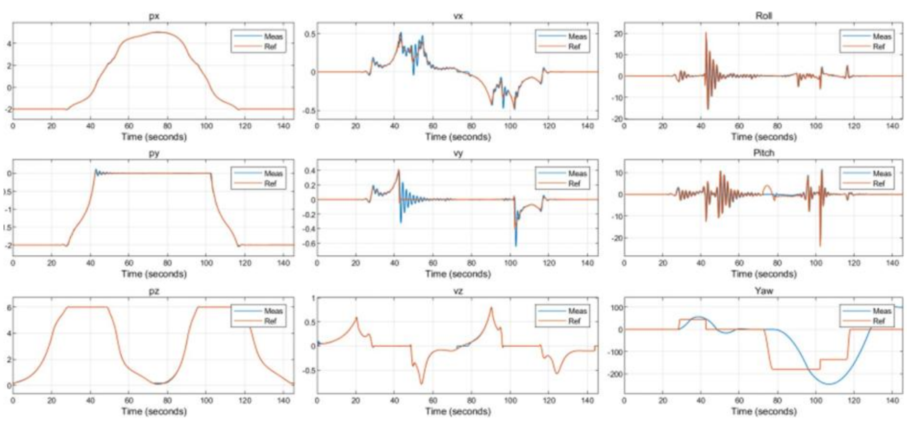

(a) Plot of positions and velocities of quadcopter chassis.

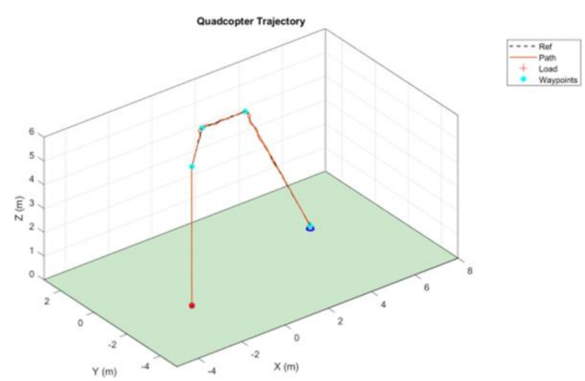

(b) Trajectory of quadcopter in 3D plane.

Fig. 13: Plot of positions and velocities of quadcopter chassis and its trajectory in 3D plane for Case I – Mars environment.

eISSN: 2583-1194

Fig. 14a shows the measured battery SOC and battery temperature. It was evident that the charge of battery drastically reduced with carrying load (simulation time: 0–75s) than without load (simulation time: 75–150s) and also for the temperature of the quadcopter battery employed. Fig. 14b shows the plot of thrust developed by the propeller system of the quadcopter. It can be seen that, the thrust required by the quadcopter was more for carrying load than the quadcopter without carrying load for the same external environment.

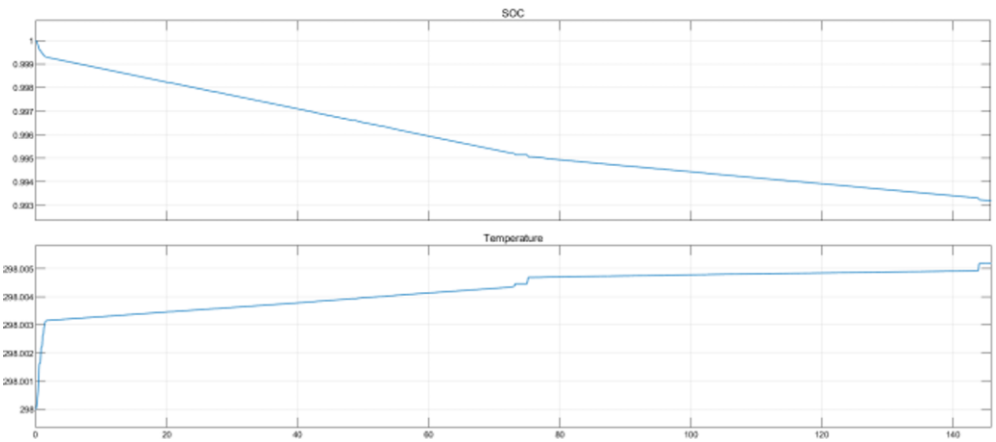

(a) Measured battery SOC and battery temperature.

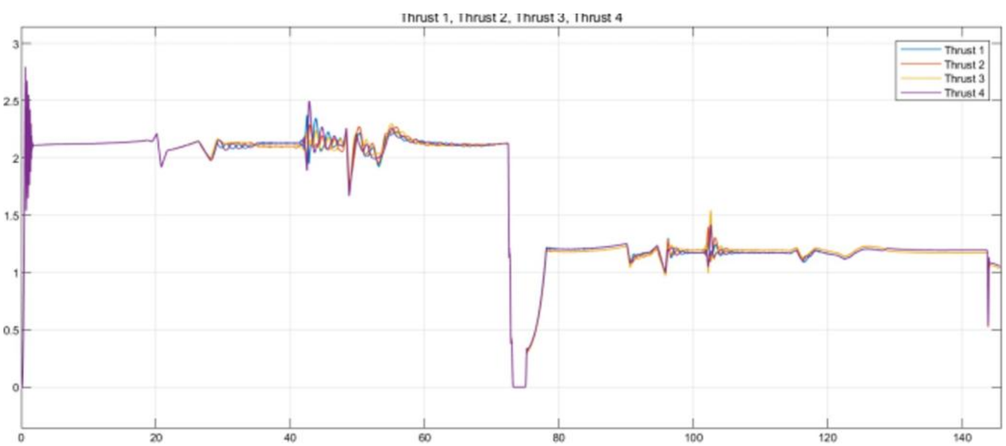

(b) Thrust developed by the propeller system.

Fig. 14: Measured battery SOC, battery temperature and thrust developed by the propeller system of quadcopter for Case I – Mars environment.

It was evident from the above quadcopter performance evaluation that it traced the predefined path for zero wind speed. It was able to reach the destination and drop off the carrying load and returned to its initial position successfully and took all commands given and interpret them effectively and little wobbling was observed.

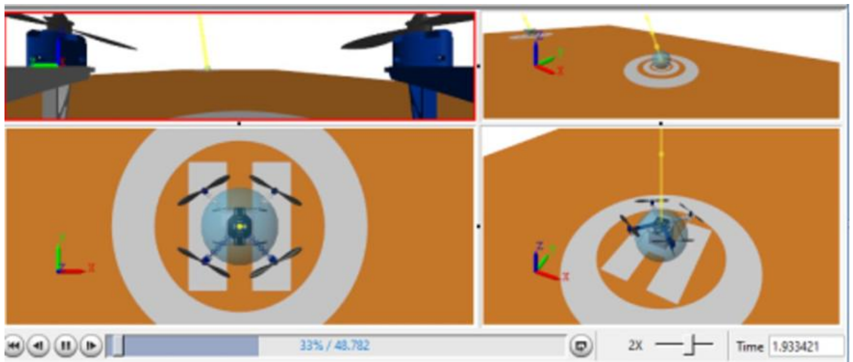

(a) Initial take-off and stabilization.

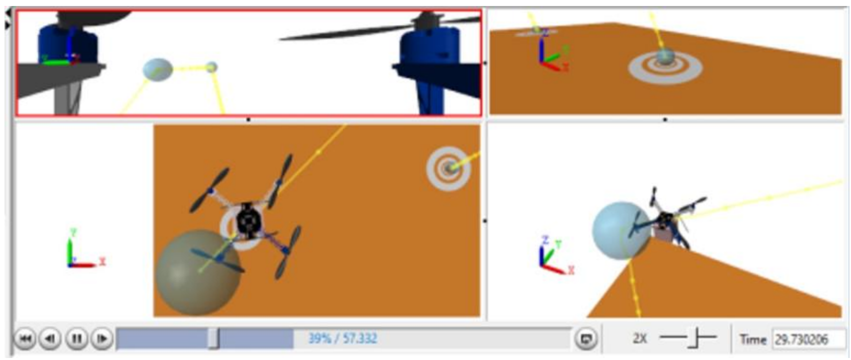

(b) Payload transportation.

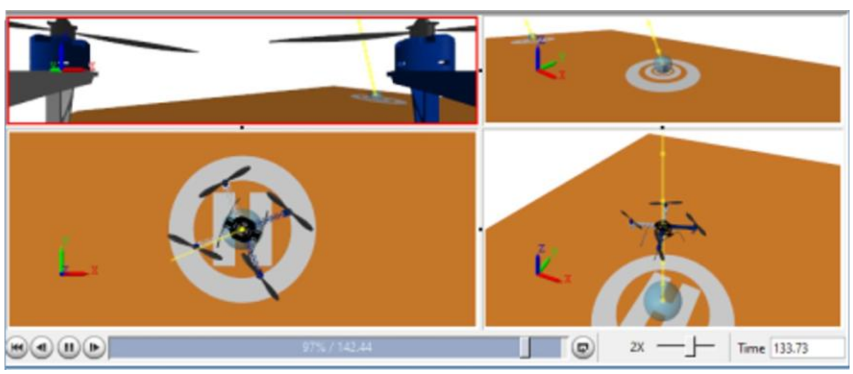

(c) Landing and mission completion.

Fig. 15: Visualization of performance of quadcopter for Case I – Mars environment.

eISSN: 2583-1194

Case II – Mars Environment:

propeller.Kthrust = 2.872;   % N

air_rho   = 0.020;   % kg/m^3

air_temperature = 273-63;   % K

gravity   = 3.721;   % m/s^2

wind_speed   = 85;   % (m/s)

trajectory_path = round_trip_2;

Fig. 16a shows the plot of positions and velocities of quadcopter chassis when the Case II control parameters was executed in which the first column plots show the position of quadcopter with respect to xyz plane, second column represents the velocity of quadcopter in xyz plane, third column represents the roll and yaw in degrees and pitch of quadcopter. The red solid line represents the reference value and blue solid line represents the measured value. Fig. 16b shows the actual quadcopter trajectory in 3D plane tracing the predefined path and can be seen that there was lot of wobbling and deviation in the actual quadcopter trajectory due to increased wind speed and was not able to reach the destination and flip out from the reference path.

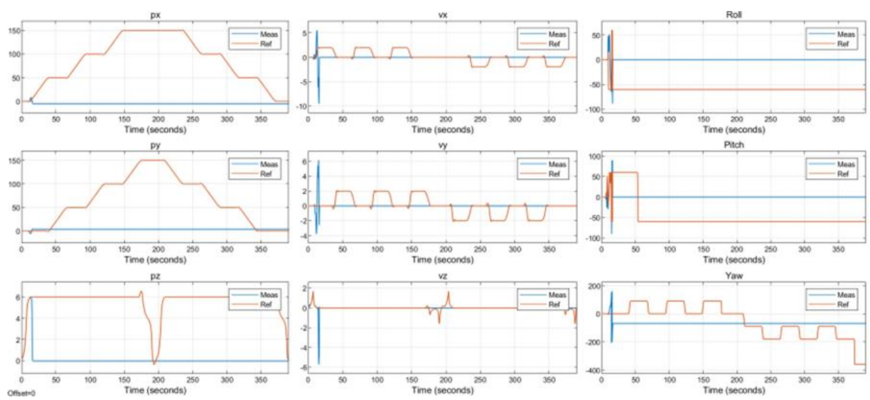

(a) Plot of positions and velocities of quadcopter chassis.

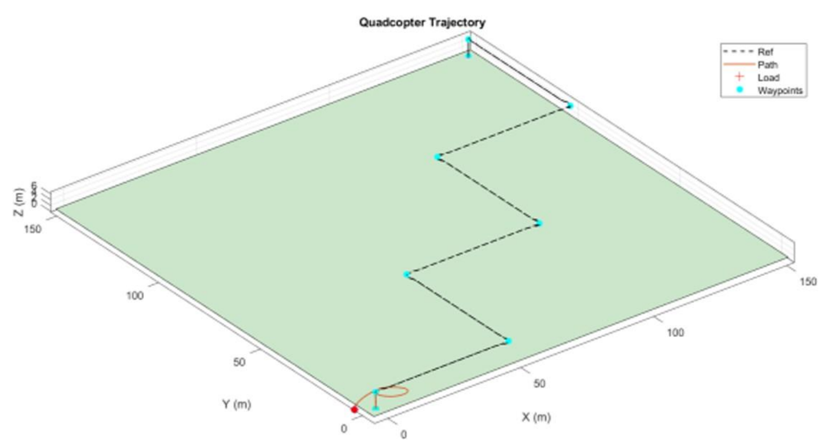

(b) Trajectory of quadcopter in 3D plane.

Fig. 16: Plot of positions and velocities of quadcopter chassis and its trajectory in 3D plane for Case II – Mars environment.

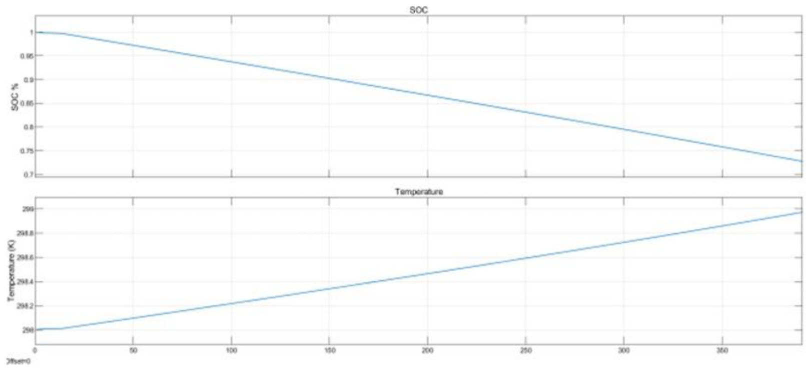

(a) Measured battery SOC and battery temperature.

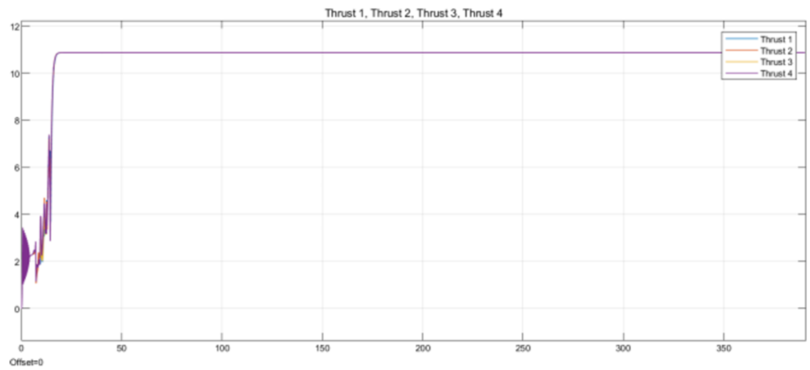

(b) Thrust developed by the propeller system.

Fig. 17: Measured battery SOC, battery temperature and thrust developed by the propeller system of quadcopter for Case II – Mars environment.

The simulation results demonstrate that the proposed quadcopter maintained acceptable trajectory tracking and flight stability under the assumed Martian environmental conditions for wind speeds up to 85 m/s. However, this observation is based exclusively on the developed simulation model and should not be interpreted as experimental validation of flight capability under such extreme atmospheric disturbances. Additional investigations incorporating high-fidelity aerodynamic models, hardware-in-the-loop testing, and experimental validation are necessary before practical operation under comparable Martian wind conditions can be confirmed.

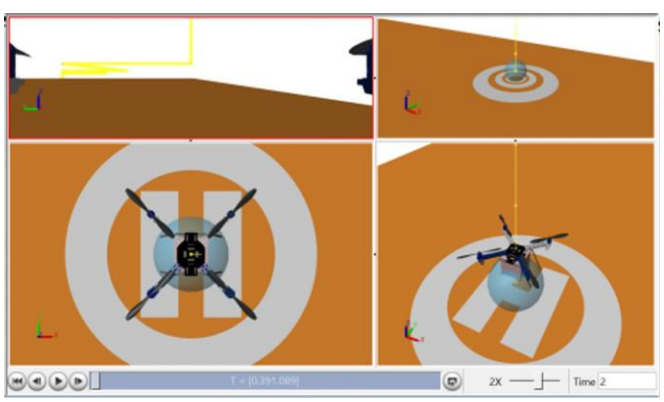

(a) Initial flight condition.

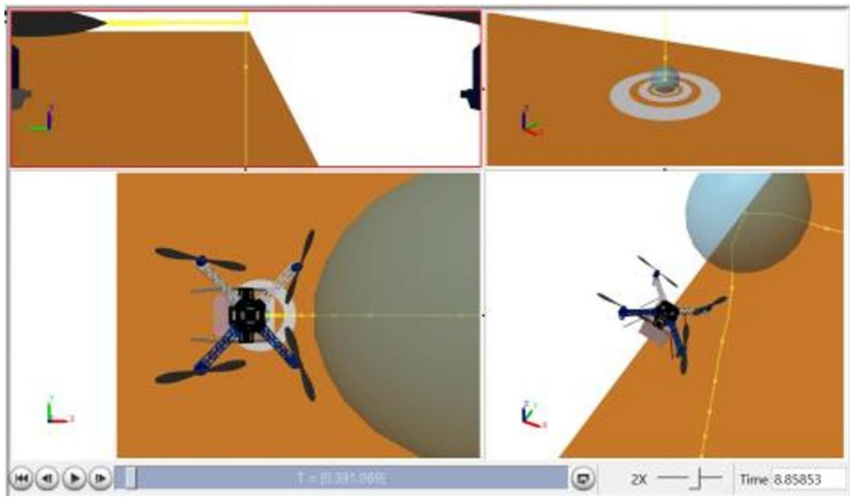

(b) Mid-flight condition.

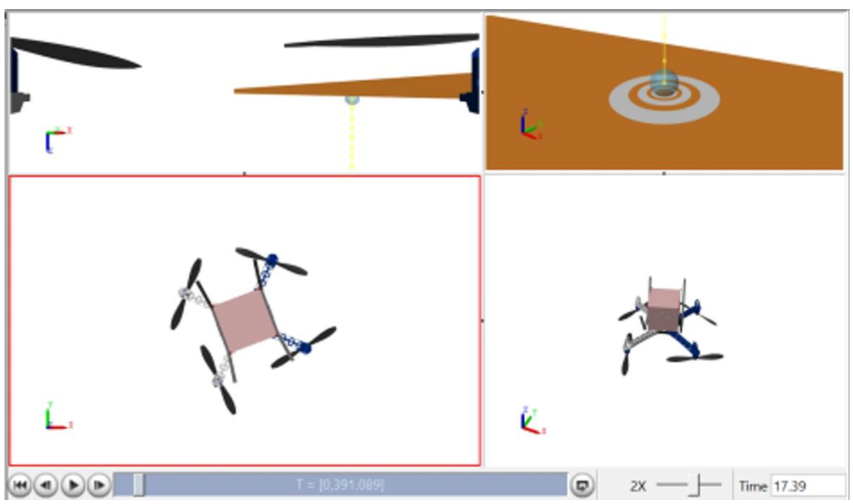

(c) Final flight condition.

Fig. 18: Visualization of performance of quadcopter for Case II – Mars environment.

4.4 Evaluation of Designed Quadcopter Propeller for Mars Environment

Figure 19 illustrates the propeller harness test conducted for the designed quadcopter under Mars atmospheric conditions. The plots show the variation of propeller speed, motor torque, and thrust with time. It can be observed that the propeller speed increases linearly from 0 to 10,000 RPM, while the corresponding torque and thrust increase gradually with rotational speed. A brief transient response is observed at the start of operation, after which the motor-propeller system reaches stable operating conditions. The generated thrust increases nonlinearly with propeller speed and reaches approximately 6.6 N at 10,000 RPM, demonstrating the capability of the propulsion system to generate sufficient lift in the low-density Martian atmosphere.

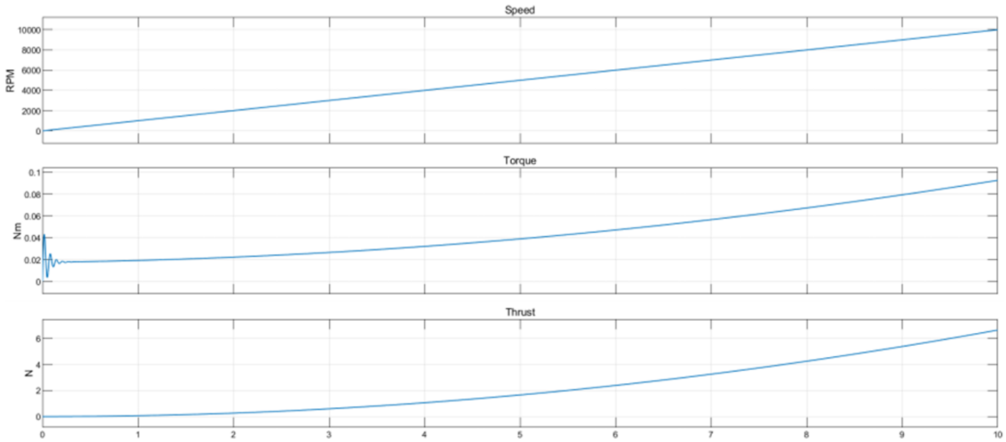

Fig. 19: Propeller harness test showing speed, torque and thrust characteristics in Mars environment.

Figure 20 shows the Simulink model developed to evaluate the maximum payload carrying capability of the designed quadcopter in the Mars environment. The model integrates the battery, motor, propeller, thrust and drag, and control subsystems to estimate the available lifting force. Based on the thrust generated by the four-propeller configuration under Martian atmospheric conditions, the maximum payload that can be safely transported was calculated to be approximately 1.428 kg. The reduction in payload capacity compared with the Earth environment is primarily due to the significantly lower atmospheric density on Mars, which requires higher thrust generation to produce the necessary lift.

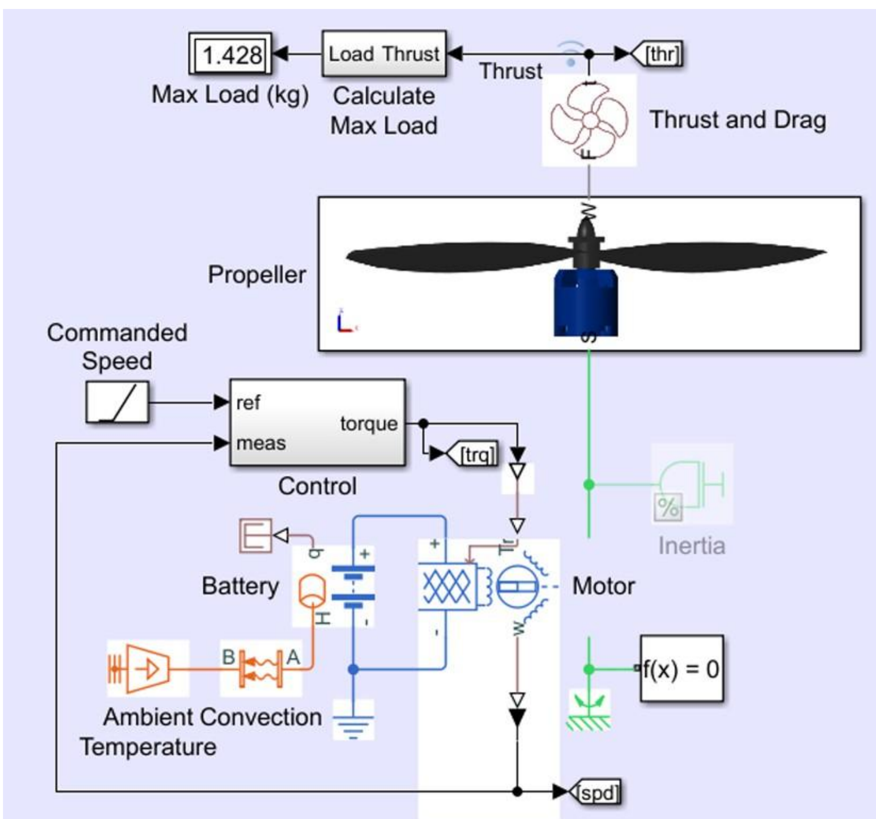

Fig. 20: Simulink model used to estimate the maximum payload carrying capacity in Mars environment.

Therefore, the propeller performance evaluation confirms that the designed quadcopter is capable of generating adequate thrust for stable flight and can carry a maximum payload of 1.428 kg in the Mars environment.

5. CONCLUSION

A unique class of unmanned aerial vehicle that may be used for a variety of purposes is the quadcopter. In this project design of body components of quadcopter using AutoCAD as well as simulation of quadcopter for planetary expedition was carried out by Simulink/MATLAB. The Linear Proportional-Derivative-Integral (PID) controller was used to control altitude, attitude, heading, and position of quadcopter in the free space. The performance evaluation of designed quadcopter was carried out for the external environment of earth and mars with varied wind speed in order to determine the suitability of designed quadcopter to collect the material samples during the planetary expedition. It was evident from the performance evaluation of designed quadcopter that the quadcopter was capable of carrying 2.136 kg of sample material in earth's environment and 1.428kg of sample material in mars environment during the planetary expedition. The capability of designed quadcopter to carry the load to the destination to drop off and return to its initial position yielded that it could complete the task up to the wind speed of 15m/s in earth's environment and up to wind speed of 85m/s in mars environment. Therefore, it can be concluded that the designed quadcopter was well suited for mars planetary expedition by taking all the commands given and interpreted them effectively to carry the maximum load of 1.428kg in the presence of wind speed up to 85m/s to collect and transport the samples from far away distance which are inaccessible for land rovers to the space shuttle landed on mars surface.

The present study is limited to simulation-based validation and does not include experimental flight testing or hardware-in-the-loop verification. In addition, structural integrity of the proposed frame has not been assessed using finite-element analysis, and higher-order aerodynamic effects such as rotor wake interactions and blade flexibility have not been considered. Furthermore, sensor noise, communication delays, actuator nonlinearities, and advanced control strategies were not explicitly investigated. Nevertheless, the developed framework provides a useful preliminary platform for evaluating the feasibility of quadcopter-based planetary exploration missions.

REFERENCES

[1] S. A. H. Mohsan, M. A. Khan, F. Noor, I. Ullah, and M. H. Alsharif, "Towards the unmanned aerial vehicles (uavs): A comprehensive review," *Drones*, vol. 6, no. 6, p. 147, 2022.

[2] G. Ononiwu, O. Onojo, O. Ozioko, and O. Nosiri, "Quadcopter design for payload delivery," *Journal of Computer and Communications*, vol. 4, pp. 1–12, 2016.

[3] M. Zemalache, L. Beji, and H. Marref, "Control of an under-actuated system: Application to a four rotors rotorcraft," in *IEEE International Conference on Robotic and Biomimetics*, 2005, pp. 404–409.

[4] G. M. Hoffmann, H. Huang, S. L. Waslander, and C. J. Tomlin, "Quadrotor helicopter flight dynamics and control: Theory and experiment," in *AIAA Guidance, Navigation and Control Conference*, 2007.

[5] H. Huang, G. M. Hoffmann, S. L. Waslander, and C. J. Tomlin, "Aerodynamics and control of autonomous quadrotor helicopters in aggressive maneuvering," in *IEEE International Conference on Robotics and Automation*, 2009, pp. 3277–3282.

[6] V. Praveen and A. S. Pillai, "Modeling and simulation of quadcopter using pid controller," pp. 7151–7158, 2015.

[7] C. Dikmen, A. Arısoy, and H. Temeltas, "Attitude control of a quadrotor," in *International Conference on Recent Advances in Space Technologies*, 2009, pp. 722–727.

[8] Z. Zuo, "Trajectory tracking control design with command-filtered compensation for a quadrotor," *IET Control Theory and Applications*, vol. 4, no. 11, pp. 2343–2355, 2010.

[9] S. Bouabdallah, A. Noth, and R. Siegwart, "Pid vs lq control techniques applied to an indoor micro quadrotor," in *IEEE/RSJ International Conference on Intelligent Robots and Systems*, 2004, pp. 2451–2456.

[10] T. Madani and A. Benallegue, "Backstepping control for a quadrotor helicopter," in *IEEE/RSJ International Conference on Intelligent Robots and Systems*, 2006, pp. 3255–3260.

[11] G. V. Raffo, M. G. Ortega, and F. R. Rubio, "An integral predictive/nonlinear h-infinity control structure for a quadrotor helicopter," *Automatica*, vol. 46, no. 1, pp. 29–39, 2010.

[12] P. Castillo, R. Lozano, and A. Dzul, "Stabilisation of a mini rotorcraft with four rotors," *IEEE Control Systems Magazine*, pp. 45–55, 2005.

[13] C. Escareno, C. Salazar-Cruz, and R. Lozano, "Embedded control of a four-rotor uav," in *American Control Conference*, 2006, pp. 3936–3941.

[14] P. Martin and E. Salaun, "The true role of accelerometer feedback in quadrotor control," in *IEEE International Conference on Robotics and Automation*, 2010, pp. 1623–1629.

[15] R. He, S. Prentice, and N. Roy, "Planning in information space for a quadrotor helicopter in a gps-denied environment," in *IEEE International Conference on Robotics and Automation*, 2008, pp. 1814–1820.

[16] B. Dasgupta and P. Choudhury, "A general strategy based on the newton–euler approach for the dynamic formulation of parallel manipulators," *Mechanism and Machine Theory*, vol. 34, no. 6, pp. 801–824, 1999.

[17] A. Salam and I. Ibraheem, "Nonlinear pid controller design for a 6-dof uav quadrotor system," *Engineering Science and Technology, an International Journal*, vol. 22, 2019.

[18] O. Hamdy and A. Elnady, "Modeling, simulation and control of quadcopter using pid controller," 2019.

[19] P. G. Fahlstrom and T. J. Gleason, *Introduction to UAV Systems*. Wiley, 2012.

[20] K. P. Valavanis and G. J. Vachtsevanos, *Handbook of Unmanned Aerial Vehicles*. Springer, 2015.

[21] NASA, "Mars exploration program," 2024. [Online]. Available: https://mars.nasa.gov

[22] "Mars fact sheet," 2024. [Online]. https://nssdc.gsfc.nasa.gov/planetary/factsheet/marsfact.html